https://doi.org/10.5194/egusphere-2023-2058
Preprint. Discussion started: 12 October 2023

Anomalous variations in stable precipitation isotopes driven by high-temperature events

Xinrui Lin[a,b,c], Guofeng Zhu[a,b,c*], Dongdong Qiu[a,b,c], Longhu Chen[a,b,c], Dehong Si[d], Linlin Ye[a,b,c], Siyu lu[a,b,c], Yinying Jiao[a,b,c], Jiawei Liu[a,b,c], Rui Li[a,b,c], Qinqin Wang[a,b,c], Jiangwei Yang[a,b,c], Wenhao Zhang[a,b,c]

[a] College of Geography and Environment Science, Northwest Normal University, Lanzhou 730070, Gansu, China

[b] Shiyang River Ecological Environment Observation Station, Northwest Normal University, Lanzhou 730070, Gansu, China

[c] Lanzhou Branch, Remote Sensing Application Center, Ministry of Agriculture and Rural Affairs

[d] Faculty of Geosciences and Environmental Engineering, Southwest Jiaotong University, Cheng Du 610000, Sichuan, China

Correspondence to: zhugf@nwnu.edu.cn

Abstract: Stable hydrogen and oxygen isotopes in atmospheric precipitation have the potential to identify abnormal weather events, and climate change will cause more intense and frequent high-temperature events, which already pose a threat to human health and the development of the global economy. Based on precipitation isotope data from 37 high-temperature events that occurred in various global regions between 2010 and 2022, this article examines the impacts of high-temperature events on stable precipitation isotopes. The results show that (1) stable precipitation isotopes are more enriched under the influence of high-temperature events than in the same month of previous years; the slope and intercept of the precipitation local meteoric water line (LMWL) are lower than in the same month of previous years and the global meteoric water line (GMWL); and the precipitation d-excess is lower than the global average. (2) Temperature is the primary meteorological factor that produces abnormal variations in precipitation isotopes under the influence of high-temperature events, and the impact of temperature on precipitation isotopes is significantly amplified ($P<0.05$). (3) Furthermore, variations in atmospheric circulation patterns, water vapor

https://doi.org/10.5194/egusphere-2023-2058
Preprint. Discussion started: 12 October 2023

transport fluxes, regional water vapor background, and surface morphology can lead to regional differences in anomalous variations in precipitation isotopes. This study reveals the impact of high temperatures on precipitation isotopes and their mechanisms, which is instructive for disentangling the influence of high-temperature events on water cycle processes. It may also offer fresh perspectives for the reconstruction of paleo-high-temperature events based on isotopes.

Keywords: High-temperature events; Water stable isotopes; Atmospheric circulation; Water vapour fluxes

1.Introduction

The increase in greenhouse gases affects global climate change and the likelihood and frequency of extreme events (Chan et al., 2020; Wehrli et al., 2019). It has been shown that global warming makes extreme weather events like storms, cold waves, and high-temperatures more likely (Patz et al., 2005; Perkins et al., 2012). The intensity, duration, and frequency of high-temperature events are predicted to rise globally in the 21st century, according to observations and predictive analyses of high-temperature events in different regions of the world. (Meehl and Tebaldi, 2004; Perkins et al., 2012). One of the most common extreme temperature events, a high temperature, is not clearly defined and is measured using different standards across the world. However, depending on the criteria used, a high temperature can be broadly characterized as an extreme event in which the daily maximum temperature exceeds a specific threshold over a continuous period of time (Barriopedro et al., 2011; Fischer et al., 2007; Perkins et al., 2012).

The high-temperature events are associated with specific circulation conditions. The anomalously convergent downwelling in the quasi-stationary upper troposphere is the most common circulation characteristic during the development of high-temperature events (Miralles et al., 2014; Seneviratne et al., 2006). Furthermore, physical conditions such as surface morphology, antecedent meteorological conditions, soil moisture, and sea surface temperature (SST) play an important role in the creation of high-temperature events (Chen and Lu, 2015; Hu et al., 2019; Wehrli et al., 2019). In general, the formation of high-temperature events at the surface is associated with

https://doi.org/10.5194/egusphere-2023-2058
Preprint. Discussion started: 12 October 2023

adiabatic heating processes during the vertical subsidence of airflow (Meehl and Tebaldi, 2004). However, horizontal airflow, in addition to vertical airflow, is capable of contributing to surface air warming via temperature advection (Chen et al., 2016; Monteiro and Caballero, 2019; Turner et al., 2022). Additionally, dry soils and changes in urban land use have an amplifying effect on high-temperature events (Barriopedro et al., 2011; Miralles et al., 2014) (Monteiro & Caballero, 2019; Patz et al., 2005). The specific magnitude of a heat event's impact hinges on the heat event's class, duration, season of occurrence, and sufficiency of public health and safety facilities (Fischer and Schär, 2010).

It is impossible to ignore how high-temperature events affect the natural water cycle. Sustained high-temperatures can cause river outflow (Barriopedro et al., 2011; Lau and Nath, 2012; Miralles et al., 2014), and meteorological conditions of low precipitation and high evaporation during high-temperature processes will lead to drought disasters (Miralles et al., 2014). However, the impact of high-temperature events on atmospheric precipitation processes is unknown. Water-stable isotopes are natural tracers that exist in a variety of water bodies and can be used to track water cycling processes in the Earth's system. Stable hydrogen and oxygen isotopes can be utilized for assessing evapotranspiration distribution (Sprenger et al., 2016), soil water transport (Zhu et al., 2022a), and water absorption by plants (Evaristo et al., 2015). Moreover, the hydrogen and oxygen stable isotopes can be used to assess how much circulating water contributes to precipitation (Li et al., 2019) and to examine how human activities affect the processes involved in the water cycle (Kathayat et al., 2021; Zhu et al., 2021). As a result, it is necessary to investigate the impact of the high-temperature events on atmospheric precipitation processes by examining their influence on stable precipitation isotopes.

Precipitation is the product of the condensation of atmospheric water vapor, and it contains a wealth of information about weather and climate change (Dansgaard, 1964; Gat and Dansgaard, 1972). The isotopic composition of the condensing parent vapor and temperature are two key factors controlling the stable precipitation isotopes (Ingraham, 1998). Temperature determines the fractionation coefficient of hydrogen

https://doi.org/10.5194/egusphere-2023-2058
Preprint. Discussion started: 12 October 2023

and oxygen stable isotopes, which therefore responds sensitively to changes in temperature (Friedman, 1953; Gat, 1996). The "temperature effect" is a positive correlation between temperature and precipitation stable isotope values that exhibits both temporal and spatial variations and is typically more pronounced in areas or seasons with significant temperature gradients (Gat and Carmi, 2001). Thus, the abnormal changes in weather systems and atmospheric circulation patterns can be reflected in stable precipitation isotopes. For instance, stable precipitation isotopes under the control of low-pressure systems are more depleted than other precipitation (Bailey et al., 2015; Wang et al., 2017). The temperature and isotopic composition of condensing parent vapor will be greatly altered by specific meteorological conditions and atmospheric circulation patterns; thus, stable precipitation isotopes are available to track the impacts of high-temperature events on atmospheric precipitation processes.

This research is based on 37 high-temperature events in different regions of the globe from 2010 to 2022, using 1233 precipitation isotope data from high-temperature events and non-high-temperature events in the same period of previous years, and is devoted to the following questions: (1) Reveal the processes and mechanisms by which high-temperature events affect the stable isotopes of precipitation. (2) Whether the changes in stable precipitation isotopes can be used to identify high-temperature events? This study can reveal the process and mechanism of anomalous changes in precipitation isotopes under the influence of high-temperature events, and it can also provide reference materials for the reconstruction of palaeo-high-temperature events based on stable isotopes.

2. Materials and methods

2.1 Data sources

2.1.1 Precipitation isotopes

In this study, we used monthly precipitation isotope data from the Global Precipitation Isotope Network (GNIP) (https://nucleus.iaea.org/wiser/index.aspx) and measured precipitation isotope data. Based on 37 global records of high-temperature events from 2010 to 2022 (Table 1), we chose 70 GNIP sites and 11 sites with

https://doi.org/10.5194/egusphere-2023-2058
Preprint. Discussion started: 12 October 2023

measured data representing precipitation isotopes for high-temperature events (Table 1). The measured data sites collected 257 daily precipitation isotope data, while the GNIP sites collected a total of 976 monthly stable precipitation isotope data. We converted daily precipitation isotope data into precipitation-weighted monthly averages with meteorological data using the algorithm below:

$$\delta = \frac{\sum_{i=1}^{n} Pi\delta i}{\sum_{i=1}^{n} Pi} \tag{1}$$

Where, Pi denotes daily precipitation (mm), and δi denotes eithter δ^2H (‰) or δ^{18}O (‰).

Table 1 Basic information on sampling points (HTs stands for High-temperature Events)

Sampling station	Latitude (°N)	Longtitude (°E)	Altitude (m)	Date sources	Period	High-temperature Events
Baoji	34.39	107.29	561	Measured data	2020-2023	HTs in southeastern Shanxi Province in June 2021
Chibi	29.72	113.9	36	Measured data	2021-2023	HTs in Hubei Province in June 2021
Gaotai	39.37	99.82	1348	Measured data	2020-2023	HTs in Northwest China in July 2021
Guangzhou	23.21	113.48	66	Measured data	2021-2023	HTs in South China in July 2022
Jinta	39.98	98.88	1271	Measured data	2021-2023	HTs in Northwest China in July 2021
Jiuquan	39.72	98.49	1483	Measured data	2021-2023	HTs in Northwest China in July 2021
Taizhou	29.07	119.64	44	Measured data	2020-2023	HTs in southern China in September 2021
Weifang	36.69	119.18	30	Measured data	2021-2023	HTs in northern China in June 2022
Xi'an	34.33	108.72	387	Measured data	2020-2023	HTs in southeastern Shanxi Province in June 2021
Xinyang	32.13	114.08	97	Measured data	2021-2023	HTs in northern China in June 2022
Zhangye	38.93	100.43	1485	Measured data	2021-2023	HTs in Northwest China in July 2021
Adelaide	-34.93	138.58	43.00	GNIP	1962-2014	HTs in Australia in January 2010
Alor Star	6.20	100.40	5.00	GNIP	1994-2016	HTs in Malaysia in April 2016 and March 2016
Ancona-Monte D'ago	43.59	13.52	170.00	GNIP	2006-2018	HTs in Europe in July, August 2015 and August 2017
Armagh Observatory	54.35	-6.65	64.00	GNIP	2010-2021	HTs in Europe in August 2017

https://doi.org/10.5194/egusphere-2023-2058
Preprint. Discussion started: 12 October 2023

Artern	51.37	11.29	164.00	GNIP	2003-2014	HTs in western Europe in April 2011 and July 2010
Avignon	43.91	4.89	33.00	GNIP	2010-2021	HTs in Europe in August 2017
Avignon	43.91	4.89	33.00	GNIP	2005-2013	HTs in western Europe in July 2010 and August 2017
Bad Salzuflen	52.10	8.75	135.00	GNIP	2005-2013	HTs in western Europe in July 2010
Bakurlani	41.73	43.52	1665.00	GNIP	2009-2020	HTs in Georgia in August 2010
Bangkok	13.73	100.50	2.00	GNIP	2000-2012	HTs in Southeast Asia in March 2010
Belo Horizonte-cdtn	-19.87	-43.97	857.00	GNIP	2009-2019	HTs in Brazil in April 2010, December 2016 and December 2018
Bonner lake	49.38	-82.12	245.00	GNIP	1998-2010	HTs in Canada in July 2010
Boulder	40.01	-105.27	1660.00	GNIP	2009-2015	HTs in the United States in May 2011, June, July 2012 and June 2016
Braunschweig	52.29	10.45	81.00	GNIP	2003-2014	HTs in Europe in July 2010 and April, May 2011
Cameron Highlands	4.47	101.38	1430.00	GNIP	1994-2016	HTs in Malaysia in March and April 2016
Cestas-Pierroton	44.74	-0.77	59.00	GNIP	2005-2013	HTs in western Europe in July 2010,April and May 2011, and August 2017
Chapais	49.82	-74.97	381.10	GNIP	1998-2010	HTs in Canada in July 2010
Charlottetown	46.29	-63.12	48.50	GNIP	2017-2021	HTs in Canada in July 2018
Cheongju	36.62	127.46	62.00	GNIP	2000-2018	HTs in South Korea in July and September 2011, August 2016, and August 2018
Cobar	-31.48	145.83	252.00	GNIP	2006-2014	HTs in Australia in January 2013
Erlangen	49.60	11.01	270.00	GNIP	2010-2021	HTs in Europe in August 2017
Espoo	60.18	24.83	30.00	GNIP	2010-2021	HTs in Europe in August 2017
Graechen-ST. Niklaus	46.20	7.84	1550.00	GNIP	2010-2021	HTs in central Europe in June 2019
Grimsel	46.57	8.33	1950.00	GNIP	2010-2021	HTs in central Europe in June 2019
Groningen	53.23	6.55	1.00	GNIP	2003-2014	HTs in Europe in April and May 2011
Havana	23.05	-82.22	137.00	GNIP	2002-2018	HTs in Cuba in April 2011
Hof-Hohensass	50.31	11.88	565.00	GNIP	2005-2015	HTs in Europe in May 2011
Hongseong	36.56	126.64	62.00	GNIP	2017-2021	HTs in South Korea in August 2016
Islamabad-Nilore	33.66	73.27	575.00	GNIP	1992-2021	HTs in Pakistan in May 2010, April, May, and August 2017

https://doi.org/10.5194/egusphere-2023-2058
Preprint. Discussion started: 12 October 2023

Johor Bahru	1.60	103.67	35.00	GNIP	1996-2016	HTs in Malaysia in March and April 2016
Kota Bahru	6.17	102.28	7.00	GNIP	2000-2016	HTs in Malaysia in March and April 2016
Kuala Lumpur	2.88	101.78	26.00	GNIP	1994-2016	HTs in Malaysia in March and April 2016
Kuala Terengganu	5.38	103.10	10.00	GNIP	1995-2016	HTs in Malaysia in March and April 2016
Kuantan	3.78	103.33	1.00	GNIP	2010-2016	HTs in Malaysia in March 2016
Kuopio	62.89	27.63	116.00	GNIP	2005-2013	HTs in western Europe in July 2010
Leon Virgen Del Camino	42.59	-5.65	916.00	GNIP	2003-2018	HTs in Europe in August 2015
Locarno	46.17	8.79	379.00	GNIP	2010-2021	HTs in central Europe in June 2019
Madrid-Retiro	40.41	-3.68	667.00	GNIP	2003-2018	HTs in Europe in August 2015
Mellingen	46.73	8.19	632.00	GNIP	2010-2021	HTs in central Europe in June 2019
Melbourne	-37.82	144.97	28.00	GNIP	1962-2014	HTs in Australia in January 2010
Mildura	-34.24	142.09	55.00	GNIP	2006-2014	HTs in Australia in January 2010
Monte Conero	43.55	13.60	530.00	GNIP	2006-2018	HTs in Europe in July 2015
Murcia	38.00	-1.17	61.00	GNIP	2003-2018	HTs in Europe in July and August 2015
Ndola	-13.00	28.65	1331.00	GNIP	2006-2017	HTs in South Africa in January 2016
Noguera de albarracin	40.46	-1.60	1449.00	GNIP	2003-2018	HTs in Europe in July and August 2015
Nyon	46.40	6.23	436.00	GNIP	2010-2021	HTs in central Europe in June 2019
Orem	40.28	-111.71	1401.00	GNIP	2015-2021	HTs in the United States in August 2016, July 2017, and July 2018
Orléans-la-source	47.83	1.94	109.00	GNIP	2003-2014	HTs in Europe in July 2010, April, May, 2011, and August 2012
Ottawa	45.32	-75.67	114.00	GNIP	2003-2018	HTs in Canada in July 2010 and July 2018
Prague	50.12	14.39	184.00	GNIP	2010-2021	HTs in Europe in August 2017
Rio Claro	-22.40	-47.54	614.50	GNIP	2013-2021	HTs in Brazil in April 2010, December 2016, and December 2018
Rio Cuarto	-33.11	-64.25	435.00	GNIP	2007-2020	HTs in Argentina in January 2010
Rovaniemi	66.50	25.76	107.00	GNIP	2005-2013	HTs in western Europe in July 2010
Santander	43.49	-3.80	52.00	GNIP	2005-2013	HTs in western Europe in July 2010
Seehausen	52.89	11.73	21.00	GNIP	2003-2014	HTs in Europe in July 2010, May and April 2011
Sevelen	47.12	9.49	450.00	GNIP	2010-2021	HTs in central Europe in June 2019

https://doi.org/10.5194/egusphere-2023-2058
Preprint. Discussion started: 12 October 2023

St. Gallen	47.43	9.40	779.00	GNIP	2010-2021	HTs in central Europe in June 2019
Stuttgart	48.83	9.20	314.00	GNIP	2003-2014	HTs in Europe in April and May 2011
Sydney	-33.95	151.17	3.00	GNIP	2006-2014	HTs in Sydney in February 2011
Tbllisi	41.75	44.77	427.00	GNIP	2009-2020	HTs in Georgia in August 2010
Tortosa	40.82	0.49	50.00	GNIP	2008-2015	HTs in Europe in July 2010 and August 2012
Trier	49.75	6.66	265.00	GNIP	2005-2013	HTs in western Europe in July 2010
Tucson	32.24	-110.94	753.00	GNIP	1996-2017	HTs in the United States in June 2012, June, and August 2016
Valentla	51.93	-10.25	9.00	GNIP	2003-2014	HTs in Europe in July 2010, April 2011, and August 2017
Wagga Wagga	-35.16	147.46	212.00	GNIP	2006-2014	HTs in Australia in January 2010 and January 2013
Wallingford	51.60	-1.10	48.00	GNIP	2003-2014	HTs in Europe in July 2010, April and May 2011, and August 2017
Wasserkuppe Rhoen	50.50	9.94	921.00	GNIP	2003-2014	HTs in Europe in July 2010, April and May 2011
Wuerzburg	49.77	9.96	268.00	GNIP	2003-2014	HTs in Europe in April 2011
Zaragoza Aeropuerto	41.66	-1.00	263.00	GNIP	2003-2018	HTs in Europe in July and August 2015
Zittau	50.90	14.80	240.00	GNIP	2010-2021	HTs in Europe in August 2017

2.1.2 Other data

The records of high-temperature events were obtained from the National Climate Center (NCC) of the China Meteorological Administration (CMA) (http://cmdp.ncc-cma.net/), which provides records of extreme weather events in China and the world. Meteorological data corresponding to monthly precipitation isotopes were obtained from GNIP, and daily meteorological data corresponding to measured data were obtained from the US National Centers for Environmental Information's Global Historical Climatology Network-Daily (GHCN-Daily), Version 3 (https://www.ncei.noaa.gov/access/search/data-search/daily-summaries). Additionally, 2.5° × 2.5° spatially resolved reanalyzed meteorological data from the National Center for Environmental Prediction/National Center for Atmospheric Research (http://www.esrl.noaa.gov) were used to calculate water vapor fluxes.

2.2 Analysis methods

2.2.1 Sampling and laboratory analysis

For precipitation sampling, we deployed 11 precipitation sampling sites in China

https://doi.org/10.5194/egusphere-2023-2058
Preprint. Discussion started: 12 October 2023

equipped with standard funnel rain collectors from 2020 to 2022. Following every precipitation event, we immediately put the samples into polyethylene plastic bottles, wrapped them with waterproof tape, and then frozen them. For solid precipitation samples, we initially put them in a ziplock bag made of plastic, and once the solid samples melted, we transferred them into sample vials and sealed them for freezing (Zhu et al., 2022b). Furthermore, after sampling, we recorded the start and end times of precipitation events, precipitation types, and precipitation amounts. The samples were all transferred to Northwestern Normal University's Isotope Laboratory for measuring the stable isotope values of hydrogen and oxygen in precipitation using a DLT-100 liquid water isotope analyzer (developed by Los Gatos Research Company), and the results of the analyses were expressed in thousandths of a difference relative to the Vienna Standard Mean Ocean Water (VSMOW) (Craig, 1961):

$$\delta_{sample}(‰) = \left[\left(\frac{R_{sample}}{R_{v-smow}}\right) - 1)\right] \times 1000 \tag{2}$$

Where R_{sample} is the ratio of heavy isotopes to light isotopes in a water sample, and the isotope ratios of δ^2H and $\delta^{18}O$ are $^1H/^2H$ and $^{18}O/^{16}O$, respectively, and $R_{V\text{-}SMOW}$ is the isotope ratio of the Vienna Standard Mean Ocean Water.

2.2.2 Water vapour flux

To identify changes in the direction of water vapor transport and its transport amount under the influence of high-temperature events, we calculated the water vapor fluxes for the months of the high-temperature events, which are given in the following formula:

$$\vec{Q} = \frac{1}{g}\int_{P_s}^{P_t}(\vec{v}\,q)dp = \frac{1}{g}\int_{P_s}^{P_t}(v\mathrm{u})qdp \tag{3}$$

In the above formula, $\vec{Q}$ is water vapor flux and its uint is $kg \cdot m^{-1} \cdot s^{-1}$, q is specific humidity ($kg \cdot kg^{-1}$). P_s is the surface air pressure, P_t is the top air pressure, u and v are the zonal wind component and the meridional wind component, respectively ($m \cdot s^{-1}$), g is the acceleration of gravity ($m \cdot s^{-1}$).

3. Results and analyses

https://doi.org/10.5194/egusphere-2023-2058
Preprint. Discussion started: 12 October 2023

3.1 The variation of precipitation isotopes under the influence of high-temperature events

Under natural conditions, stable isotopes of precipitation exhibit spatial variations of depletion from low to high latitudes and temporal variations of enrichment in summer and depletion in winter due to geographical factors (Clark and Fritz, 1997; Craig, 1961). However, extreme climatic events, such as high-temperature events, have an impact on precipitation isotopes' natural characteristics, which results in an enrichment of precipitation isotopes during high-temperature event months (Fig. 1). This enrichment may be related to the "temperature effect" of precipitation isotopes and the "below-cloud effects." Specifically, stable precipitation isotopes are more enriched in the month of the high-temperature event than over the same period in previous years in different regions of the world. The enrichment of precipitation isotopes under the influence of high-temperature events occurs from low to high latitudes but is more pronounced in the middle and high latitudes. The Southeast Asian heatwave in March 2010 (Figure 1a and b), the Malaysian heatwave in April 2016 (Figure 1a and b), and the Cuban heatwave in April 2011 (Figure 1e and f) were heatwave events in low-latitude regions. From the figures, it can be observed that precipitation isotopes themselves are more enriched at low latitudes, and the difference between precipitation isotopes during high-temperature event months and non-high-temperature event months is small. On the other hand, in middle- and high-latitude regions, there is a great difference between the precipitation isotopes during high-temperature event months and non-high-temperature event months. This suggests that the impact of high-temperature events on stable precipitation isotopes varies across different parts of the world.

https://doi.org/10.5194/egusphere-2023-2058
Preprint. Discussion started: 12 October 2023

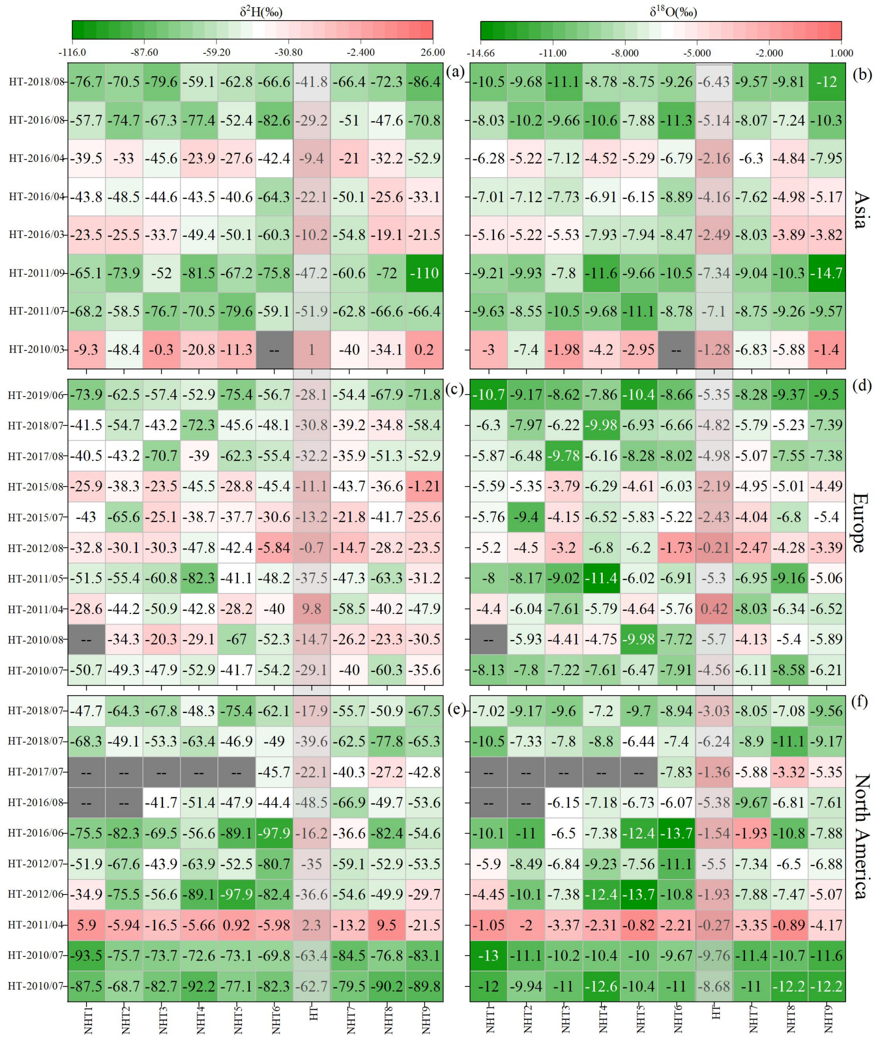

Figure 1. Differences in stable precipitation isotopes between months of high-temperature events and the same period in previous years from 2010 to 2022 for (a-b) Asia, (c-d) Europe, and (e-f) North America. In the figure, HTs represent high-temperature events, and NHTs represent non-high-temperature events. The gray rectangle represents the stable isotope of precipitation for high-temperature events.

3.2 The variation of local meteoric water lines under the influence of high-temperature events

To measure changes in precipitation isotope fractionation under the influence of high-temperature events, we analyzed differences in the local meteoric water lines

https://doi.org/10.5194/egusphere-2023-2058
Preprint. Discussion started: 12 October 2023

(LMWL) between high-temperature events and non-high-temperature events in different regions of the globe. The slope of the LMWL is related to temperature and evaporation degrees. In the context of drought and high temperatures, the slope of the LMWL is lower than the global average (8) (Clark and Fritz, 1997). The intercept of the LMWL is controlled by relative humidity, and lower intercepts indicate that precipitation experiences more kinetic fractionation during precipitation (Ingraham, 1998). The slope and intercept of the LMWL under the influence of high-temperature events ($\delta^2H=6.69\delta^{18}O+1.43$ $R^2=0.89$) are lower than the global meteoric water line (GMWL) ($\delta^2H=8\delta^{18}O+10$ $R^2=1.00$), indicating that the precipitation isotopes suffer evaporation and dynamic fractionation. The slope and intercept of the LMWL under the influence of high-temperature events are lower than those of non-high-temperature events in the same period of previous years ($\delta^2H=7.77\delta^{18}O+7.35$ $R^2=0.95$), which suggests an increased evaporation and dynamic fractionation process of precipitation isotopes under the influence of high-temperature events (Figure 2g). There are differences in the LMWL under the influence of high-temperature events in different regions of the world. In Europe and North America, there are noticeable differences in the slopes and intercepts of LMWL between high-temperature events and non-high-temperature events in the same period of previous years (Figures 2b, c), whereas in Asia, South America, and Oceania, the slopes and intercepts of LMWL are only slightly different for high-temperature event months than those for non-high-temperature event months (Figures 2a, d, and f). These findings demonstrate variations in the evaporation fractionation of precipitation isotopes during high-temperature events in different regions, which may be related to the causes of high-temperature events and land area factors. Furthermore, the slope of the LMWL in the southern hemisphere during summer is close to or higher than the GMWL (Figure 2d–e), whereas the LMWL in the northern hemisphere is all lower than the GMWL (Figure 2a–c). This implies that stable precipitation isotopes in the northern hemisphere during the summer are more influenced by evaporation than those in the southern hemisphere.

https://doi.org/10.5194/egusphere-2023-2058
Preprint. Discussion started: 12 October 2023

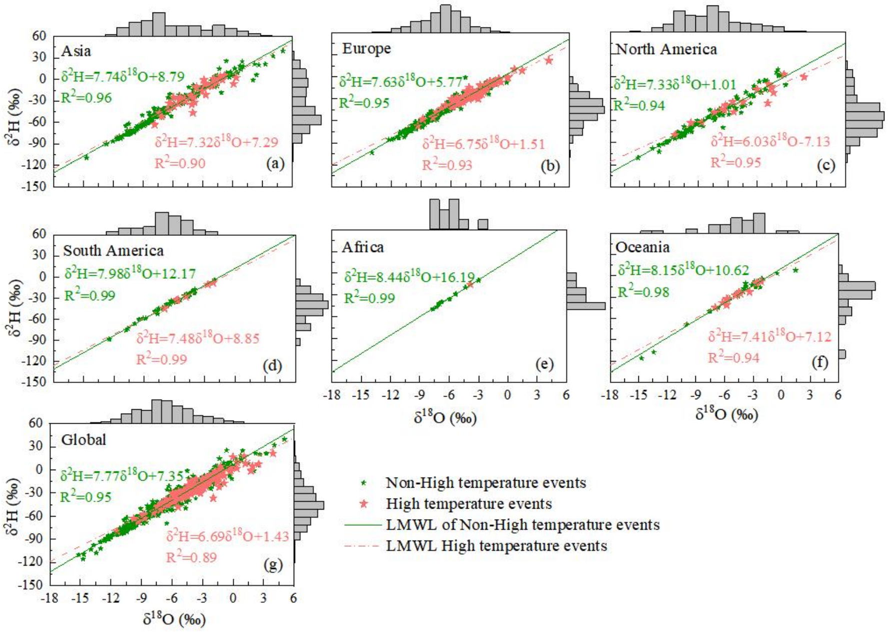

Figure 2 The differences of the LMWL under the influence of high-temperature events and in the same period of previous years (a–f) represent different continents, and (g) is the global average.

3.3 The variation of precipitation d-excess under the influence of high-temperature events

Precipitation d-excess (d-excess=$\delta^2H-8\delta^{18}O$) is a powerful tool for inferring the water vapor source and non-equilibrium fractionation of isotopes. This is because, during equilibrium fractionation, d-excess counteracts the covariation of hydrogen and oxygen stable isotope compositions and changes only slightly (Dansgaard, 1964). However, during non-equilibrium processes, the difference in molecular mass of hydrogen and oxygen causes kinetic fractionation, resulting in a decrease in d-excess (Carroll et al., 2022). The decrease of d-excess from its initial state in the precipitation process represents evaporation or sublimation of the precipitation (Clark and Fritz, 1997). We compared the changes in precipitation d-excess between high-temperature events and non-high-temperature events across various continents in order to assess the changes in the water vapor source and non-equilibrium fractionation of isotopes under the influence of high-temperature events. The average d-excess of precipitation

https://doi.org/10.5194/egusphere-2023-2058
Preprint. Discussion started: 12 October 2023

under the influence of global high-temperature events was 6.48 ‰, while the average d-excess of precipitation during non-high-temperature events in the same period was 8.27 ‰ (Figure 3). This suggests that there is an increased kinetic fractionation of precipitation isotopes under the influence of high-temperature events. The study also found that, with the exception of Africa, the mean d-excess of precipitation on other continents during high-temperature events was lower than that during non-high-temperature events in the same period. In Africa and South America, the d-excess values are higher under the influence of high-temperature events, which may be related to the water vapor source, because their precipitation d-excess was also higher in the same months as previous years (Figure 3). In addition, the d-excess of precipitation in Asia and Oceania during both high-temperature events and non-high-temperature events was close to the global average (10 ‰), and the d-excess values of precipitation during high-temperature events and non-high-temperature events in Europe and North America were much lower than the global average (10 ‰). These findings imply that there are regional differences in the kinetic fractionation of precipitation isotopes under the influence of high-temperature events.

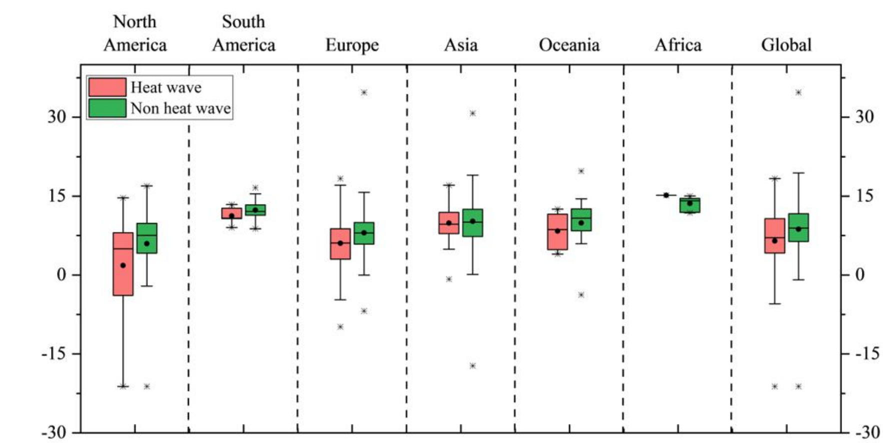

	HT	NHT	HT	NHT	HT	NHT	HT	NHT	HT	NHT	HT	NHT	HT	NHT
Max(‰)	14.68	16.94	11.25	16.6	18.34	34.71	17.1	30.76	12.52	19.76	-	15.04	18.34	34.71
Min(‰)	-21.16	-21.16	9.02	8.8	-9.84	-6.83	-0.79	-17.25	3.98	-3.76	-	11.81	-21.16	-21.16
Mean(‰)	1.82	5.96	11.25	12.34	6.05	8.03	9.89	10.21	8.37	9.91	-	13.59	6.48	8.72

Figure 3. Differences between the precipitation d-excess during high-temperature events and the same period in previous years in various regions of the world, and the variation characterization of

https://doi.org/10.5194/egusphere-2023-2058
Preprint. Discussion started: 12 October 2023

d-excess.

4. Discussion

4.1 The impact of high-temperature events on stable precipitation isotopes

4.1.1 The impacts of environmental factors changing on stable precipitation isotopes

To investigate how different environmental factors (precipitation, air temperature, water vapor pressure, latitude, and altitude) affect stable precipitation isotopes under the influence of high-temperature events. We compared the correlations between precipitation isotopes and various environmental factors (precipitation, temperature, water vapor pressure, latitude, and altitude) under the influence of high-temperature events and in the same periods of previous years (Table 2). Under the influence of high-temperature events, the precipitation $\delta^{18}O$ showed a significant negative correlation with precipitation amount ($P<0.05$), a significant positive correlation with temperature ($P<0.01$), and a significant positive correlation with water vapor pressure ($P<0.01$). However, there was no significant correlation between the precipitation $\delta^{18}O$ and latitude or altitude. The relationship between precipitation $\delta^{2}H$ under the influence of high-temperature events and various environmental factors was consistent with that of $\delta^{18}O$. Those findings suggest that precipitation, temperature, and water vapor pressure are the primary environmental factors that control the stable precipitation isotopes under the influence of high-temperature events. Furthermore, precipitation $\delta^{18}O$ correlation with temperature and water vapor pressure increased under the influence of high-temperature events, while the correlation with precipitation decreased. The information above shows that during high-temperature events, the effects of temperature and water vapor pressure on the isotopic composition of precipitation are amplified, while the effects of precipitation are diminished.

Table 2 Regression analysis and correlation coefficients of $\delta^{18}O$ and $\delta^{2}H$ with precipitation, temperature, and water vapor pressure under the influence of high-temperature events and in the same period of previous years from 2010 to 2022 (HTs is an abbreviation for high-temperature events; NHTs is for non-high-temperature events.)

	$\delta^{18}O$	$\delta^{2}H$

https://doi.org/10.5194/egusphere-2023-2058
Preprint. Discussion started: 12 October 2023

		NHTs	HTs	NHTs	HTs
P	S/‰.mm^{-1}	$\delta^{18}O=-0.01P-5.60$	$\delta^{18}O=-0.01P-3.09$	$\delta^{2}H=-0.07P-37.81$	$\delta^{2}H=-0.05P-20.67$
	r	-0.33**	-0.32**	-0.29**	-0.24*
T	S/‰.°C^{-1}	$\delta^{18}O=0.13T-9.40$	$\delta^{18}O=0.15T-7.05$	$\delta^{2}H=0.99T-65.82$	$\delta^{2}H=1.03T-47.03$
	r	0.28**	0.33**	0.27**	0.33**
e	S/‰.hPa^{-1}	$\delta^{18}O=0.06e-7.13$	$\delta^{18}O=0.06e-4.33$	$\delta^{2}H=0.66e-52.74$	$\delta^{2}H=0.79e-35.91$
	r	0.11*	0.14**	0.17**	0.28*
Lat	S/‰.°$^{-1}$	$\delta^{18}O=-0.02L-5.93$	$\delta^{18}O=0.01L-3.89$	$\delta^{2}H=-0.22L-37.97$	$\delta^{2}H=-0.04L-22.54$
	r	-0.20**	0.07	-0.26**	-0.06
Alt	S/‰.m^{-1}	$\delta^{18}O=-0.001A-6.24$	$\delta^{18}O=-0.001A-3.54$	$\delta^{2}H=-0.01A-41.33$	$\delta^{2}H=-0.004A-22.28$
	r	-0.15**	-0.07	-0.18**	-0.10

** Significantly correlated at the 0.01 level (bilateral)

* Significantly correlated at the 0.05 level (bilateral)

To further investigate the specific impact of environmental factors on precipitation isotopes under the influence of high-temperature events, we used least-squares regression to analyze the differences in the environmental effects on precipitation isotopes during high-temperature event months and non-high-temperature event months (Table 2). Under the influence of high-temperature events, the temperature effect is higher than that of non-high-temperature events in the same period of the previous years; the amount effect is lower than that of non-high-temperature events in the same period of the previous years; and the variation of precipitation $\delta^{18}O$ and $\delta^{2}H$ with the water vapor pressure is enhanced. We can see that the positive control of precipitation $\delta^{18}O$ by temperature is stronger than the negative control of precipitation and the positive control of water vapor pressure. The relationship between precipitation $\delta^{2}H$ and temperature, precipitation, and water vapor pressure is consistent with $\delta^{18}O$. This suggests that, under the influence of high-temperature events (Table 2), temperature is the dominant environmental factor affecting the precipitation isotopes, and the enrichment of stable precipitation isotopes is caused by the anomalous changes in temperature. Additionally, the higher temperature difference in mid-high latitude regions produced a stronger temperature effect, and thus the enrichment of precipitation isotopes is more pronounced in mid-high latitude regions than in low latitude regions (Clark and Fritz, 1997; Dansgaard, 1964). Overall, the enrichment of precipitation isotopes under the influence of high-temperature events is primarily

https://doi.org/10.5194/egusphere-2023-2058
Preprint. Discussion started: 12 October 2023

controlled by temperature, and regional variability in temperature effects is the fundamental factor for the regional variance of the isotopic enrichment phenomenon.

4.1.2 Impact of changes in atmospheric circulation patterns on stable precipitation isotopes

The formation of high-temperature events is related to the control of anticyclone circulation (high pressure) (Wehrli et al., 2019). Blocking high-pressure systems or warm advection transport resulting from changes in atmospheric circulation patterns can produce clear, dry, and hot meteorological conditions (Fischer and Schär, 2010; Hu et al., 2019; Schubert et al., 2014). Under the influence of high-temperature events, stable hydrogen-oxygen isotopes in precipitation show enrichment phenomena, and precipitation d-excess decreases, while the slope and intercept of LMWL also present a declining trend. This is because high-temperature events create a weather background with less precipitation and more evaporation, and the precipitation isotopes experienced a stronger evaporation process than they did during non-high-temperature events in the same periods of previous years. Figure 4 represents atmospheric circulation patterns and water vapor transport fluxes in different regions of the world during months of high-temperature events. The impacts of atmospheric circulation patterns can be classified into two categories: one is under the direct control of high-pressure systems, and the other is under the indirect influence of nearby high-pressure systems through warm advective transport (Figures 4a–d and 4i–l). In different regions of the world, under the control of high-pressure systems, the transport of water vapor from low-latitude tropical regions increases during high-temperature event months (Figures 4e–h and Figure 4m–p). Therefore, the average precipitation d-excess under the influence of high-temperature events (6.48 ‰) is lower than the global average (10 ‰) and the non-high-temperature events in the same period of previous years (8.27 ‰). This is because water vapor from low-latitude oceanic regions with relatively high humidity has a lower d-excess value (Froehlich et al., 2002; Gat et al., 2003; Gat and Carmi, 2001). In summary, the increase in low-latitude water vapor transport is one of the reasons for the decrease in the average d-excess under the influence of high-temperature events.

https://doi.org/10.5194/egusphere-2023-2058
Preprint. Discussion started: 12 October 2023

The changes in atmospheric circulation patterns will greatly modify the regional water vapor sources and the amount of water vapor transport (Gimeno et al., 2012; Wang et al., 2017). Variations in water vapor flux lead to regional differences in stable precipitation isotopes as well as in d-excess (Kino et al., 2021; Wei et al., 2018). In Asia and Oceania, high-pressure systems are primarily atmospheric circulation patterns (Fig. 4c, d, and j), and the water vapor transport flux from low latitudes is increased (Fig. 4f, h, and n) during months of high-temperature events. However, the precipitation d-excess is slightly lower than the global average (Figure 3) under the influence of high-temperature events,and the slope of the LMWL is lower than that of the GMWL (Figure 2a, f). These results illustrate that the evaporative fractionation processes in precipitation isotopes strengthen under the influence of high-temperature events in Asia and Oceania, while the alteration of water vapor transport has little impact on the precipitation d-excess. Besides, in Europe and North America, the atmospheric circulation pattern is a warm advection transport from a nearby high-pressure system under the influence of high-temperature events (Fig. 4a, b), and the water vapor transport flux from high latitudes is increasing (Fig. 4e, f). However, high-temperature events in Europe and North America are frequently accompanied by dry meteorological conditions (Barriopedro et al., 2011; Fischer et al., 2012; Hoerling et al., 2013; Schubert et al., 2014). And in warm and dry air, rapid evaporation of raindrops will result in low precipitation d-excess values and LMWL intercepts (Ingraham, 1998; Merlivat and Jouzel, 1979). Thus, in Europe and North America, the precipitation d-excess is much lower than the global average, and the intercept of the LMWL is extremely low, indicating that the below-cloud effects of precipitation isotopes were enhanced under the influence of high-temperature events. Furthermore, during months of high temperatures in South Africa, a near-surface low-pressure system transports evaporated water vapor from a series of lakes near the East African Rift Valley to South Africa. Meanwhile, a high-pressure system in the South Atlantic transports water vapor with higher d-excess values near 30°S to South Africa (Figures 4i and 4m). During high-temperature event months in South America, a high-pressure system over the South Atlantic Ocean mainly controls South America (Figures 4k-l

https://doi.org/10.5194/egusphere-2023-2058
Preprint. Discussion started: 12 October 2023

and 4o-p). Due to the influence of the Andes Mountains, the majority of South America is located on the continent's leeward side, and evaporative water vapor over land accounts for the majority of water vapor transport in the region (Jouzel et al., 2013). The leeward side of the continents has a large humidity gradient, resulting in high d-excess water vapor, while evaporated water vapor from land surfaces also has high d-excess values (Deshpande et al., 2013; Gat, 2000). Therefore, the precipitation d-excess in South America and South Africa is higher than the global average under the influence of high-temperature events. In conclusion, abnormal meteorological conditions, changes in water vapor transport fluxes, and shifts in atmospheric circulation patterns all have an impact on variations in precipitation isotopes under the influence of high-temperature events. Additionally, topography and underlying surface conditions are also important factors in regional differences in precipitation isotopes under the influence of high-temperature events.

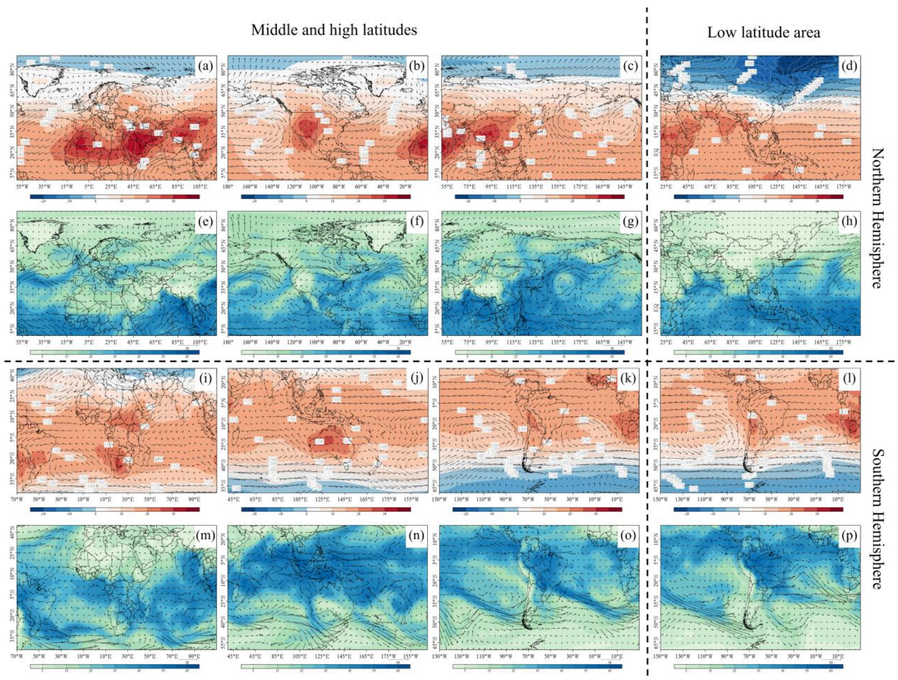

Figure 4. Atmospheric circulation pattern fields (850 hP) and water vapor flux for different regions worldwide during months of high-temperature events. Figures (a–d) represent the synthesized 850-hPa wind field (m/s), temperature field (°C), and geopotential height field (gpm) for different regional high-temperature events in the

https://doi.org/10.5194/egusphere-2023-2058
Preprint. Discussion started: 12 October 2023

Northern Hemisphere, while figures (i–l) represent the same for the Southern Hemisphere. Figures (e–h) show the water vapor flux maps for different high-temperature events in the Northern Hemisphere, and figures (m–p) depict the same for the Southern Hemisphere. In addition, (a–c), (e–g), (i–k), and (m–o) represent high-temperature events at mid- to high-latitudes, and (d), (h), (l), and (p) represent high-temperature events at low-latitudes.

4.3 Implications for paleoclimate studies

The development of a framework for understanding the response of stable water isotopes to high-temperature events can provide valuable information for reconstructing past temperature changes using ancient isotope records. Many water isotope proxies preserved in tree rings (McCarroll and Loader, 2004), lake sediments (Leng and Marshall, 2004), loess sediments (Barta et al., 2018; Kaakinen et al., 2006), and ice cores (Thompson et al., 2000) are frequently utilized to reconstruct past climate change characteristics. A high-resolution, long-time-series water isotope record is often used to restore the alternating cool-warm and dry-wet characteristics of the climate during historical periods (Johnson and Ingram, 2004). The interpretation of the palaeoisotope record hinges on the study of modern precipitation isotopes; however, it will be more challenging to correctly interpret the palaeoisotope record in these natural archives as the climate changes. According to earlier research, the long-term precipitation isotope record preserves information about warming in Central Asia (Zhu et al., 2023), and the hourly high-resolution precipitation isotope record can be used to reconstruct the evolution of extreme weather events like typhoons (Sánchez-Murillo et al., 2019; Wang et al., 2021). In addition, the isotopic composition of water vapor is a reliable indicator for tracing the water vapor source during high-temperature events (Bonne et al., 2015). Stable isotopes of precipitation will invariably undergo aberrant alterations as a result of the abrupt changes in meteorological parameters that occur during extreme weather events, such as high temperatures. However, the regulating mechanisms of high-temperature events on stable precipitation isotopes are not yet fully understood. Our current research indicates that the stable precipitation isotopes during high-temperature event months are more enriched compared to the same period in previous years, and this enrichment phenomenon has regional variations with different causes. These findings will offer

https://doi.org/10.5194/egusphere-2023-2058
Preprint. Discussion started: 12 October 2023

new insights for isotope-based reconstruction of palaeo-high-temperature events. Therefore, it is necessary to establish a framework for the control mechanism of global high-temperature events on stable precipitation isotopes, which is helpful in reconstructing past high-temperature activities in the future.

5. Conclusion

This study analyzes the abnormal variations of precipitation isotopes and their mechanisms under the influence of high-temperature events in various regions around the world based on precipitation isotope data from GNIP and sampling. The results show that stable precipitation isotopes are more enriched under the influence of high-temperature events than during the same period in previous years. This is because the influence of temperature on stable precipitation isotopes is significantly enhanced under the influence of high-temperature events. Moreover, as the temperature effect is more pronounced in regions with large temperature differences, the enrichment phenomenon of precipitation isotopes is more visible in mid- and high-latitude regions. The slope and intercept of the local meteoric water line (LMWL) under the influence of high-temperature events are significantly lower than those of the global meteoric water line (GMWL). This is because high-temperature events produce dry meteorological conditions, which lead to a stronger kinetic fractionation of precipitation isotopes. The average value of precipitation d-excess under the influence of high-temperature events is lower than the same period in previous years and the global average, which is attributed to the strong evaporation and the variation of water vapor flux. Additionally, there are regional variations in the abnormal changes in precipitation isotopes, d-excess, and LMWL as a result of the influence of atmospheric circulation patterns, water vapor transport fluxes, regional background water vapor isotope characteristics, and surface morphology. This research reveals the impact of high-temperature events on stable precipitation isotopes and their mechanisms, which is beneficial for understanding the influence of high-temperature events on the water cycle process. These findings also contribute to a more accurate interpretation of isotope records and the reconstruction of past high-temperature events in paleoclimate archives.

Conflict of Interest Statement

The authors declare no conflicts of interest.

Acknowledgements

This research was financially supported by the National Natural Science Foundation of China(41971036), the National Natural Science Foundation innovation research group science foundation of China (41421061)，Key Natural Science Foundation of Gansu Province (23JRRA698)，Key Research and Development Program of Gansu Province (22YF7NA122).

Data Availability Statement

The sampling data that support the findings of this study are available on request from https://doi.org/10.5194/essd-14-3773-2022, other isotope data can be obtained at GNIP (http://isohis.iaea.org/News.asp). Meteorological data were obtained from the US National Centers for Environmental Information's Global Historical Climatology Network-Daily (GHCN-Daily), Version 3 (https://www.ncei.noaa.gov/access/search/data-search/daily-summaries). Reanalyzed meteorological data from the National Center for Environmental Prediction/National Center for Atmospheric Research (http://www.esrl.noaa.gov).

Referencre

Bailey, H. L., Kaufman, D. S., Henderson, A. C. G., and Leng, M. J.: Synoptic scale controls on the $\delta^{18}O$ in precipitation across Beringia, Geophys. Res. Lett., 42, 4608–4616, https://doi.org/10.1002/2015GL063983, 2015.

Barriopedro, D., Fischer, E. M., Luterbacher, J., Trigo, R. M., and García-Herrera, R.:

https://doi.org/10.5194/egusphere-2023-2058
Preprint. Discussion started: 12 October 2023

The Hot Summer of 2010: Redrawing the Temperature Record Map of Europe, Science, 332, 220–224, https://doi.org/10.1126/science.1201224, 2011.

Barta, G., Bradák, B., Novothny, Á., Markó, A., Szeberényi, J., Kiss, K., and Kovács, J.: The influence of paleogeomorphology on the stable isotope signals of paleosols, Geoderma, 330, 221–231, https://doi.org/10.1016/j.geoderma.2018.05.033, 2018.

Bonne, J.-L., Steen-Larsen, H. C., Risi, C., Werner, M., Sodemann, H., Lacour, J.-L., Fettweis, X., Cesana, G., Delmotte, M., Cattani, O., Vallelonga, P., Kjaer, H. A., Clerbaux, C., Sveinbjörnsdóttir, Á. E., and Masson-Delmotte, V.: The summer 2012 Greenland heat wave: In situ and remote sensing observations of water vapor isotopic composition during an atmospheric river event, J. Geophys. Res. Atmospheres, 120, 2970–2989, https://doi.org/10.1002/2014JD022602, 2015.

Carroll, R. W. H., Deems, J., Sprenger, M., Maxwell, R., Brown, W., Newman, A., Beutler, C., and Williams, K. H.: Modeling Snow Dynamics and Stable Water Isotopes Across Mountain Landscapes, Geophys. Res. Lett., 49, https://doi.org/10.1029/2022GL098780, 2022.

Chan, D., Cobb, A., Zeppetello, L. R. V., Battisti, D. S., and Huybers, P.: Summertime Temperature Variability Increases With Local Warming in Midlatitude Regions, Geophys. Res. Lett., 47, https://doi.org/10.1029/2020GL087624, 2020.

Chen, F., Jia, J., Chen, J., Li, G., Zhang, X., Xie, H., Xia, D., Huang, W., and An, C.: A persistent Holocene wetting trend in arid central Asia, with wettest conditions in the late Holocene, revealed by multi-proxy analyses of loess-paleosol sequences in Xinjiang, China, Quat. Sci. Rev., 146, 134–146, https://doi.org/10.1016/j.quascirev.2016.06.002, 2016.

Chen, R. and Lu, R.: Comparisons of the Circulation Anomalies Associated with Extreme Heat in Different Regions of Eastern China, J. Clim., 28, 5830–5844, https://doi.org/10.1175/JCLI-D-14-00818.1, 2015.

https://doi.org/10.5194/egusphere-2023-2058
Preprint. Discussion started: 12 October 2023

Clark, I. D. and Fritz, P.: Environmental isotopes in hydrogeology, CRC Press/Lewis Publishers, Boca Raton, FL, 328 pp., 1997.

Craig, H.: Isotopic Variations in Meteoric Waters, Sci. New Ser., 133, 1702–1703, 1961.

Dansgaard, W.: Stable isotopes in precipitation, Tellus, 16, 436–468, https://doi.org/10.1111/j.2153-3490.1964.tb00181.x, 1964.

Deshpande, R. D., Maurya, A. S., Kumar, B., Sarkar, A., and Gupta, S. K.: Kinetic fractionation of water isotopes during liquid condensation under super-saturated condition, Geochim. Cosmochim. Acta, 100, 60–72, https://doi.org/10.1016/j.gca.2012.10.009, 2013.

Evaristo, J., Jasechko, S., and McDonnell, J. J.: Global separation of plant transpiration from groundwater and streamflow, Nature, 525, 91–94, https://doi.org/10.1038/nature14983, 2015.

Fischer, E. M. and Schär, C.: Consistent geographical patterns of changes in high-impact European heatwaves, Nat. Geosci., 3, 398–403, https://doi.org/10.1038/ngeo866, 2010.

Fischer, E. M., Seneviratne, S. I., Lüthi, D., and Schär, C.: Contribution of land-atmosphere coupling to recent European summer heat waves, Geophys. Res. Lett., 34, L06707, https://doi.org/10.1029/2006GL029068, 2007.

Fischer, E. M., Rajczak, J., and Schär, C.: Changes in European summer temperature variability revisited: CHANGES IN TEMPERATURE VARIABILITY, Geophys. Res. Lett., 39, n/a-n/a, https://doi.org/10.1029/2012GL052730, 2012.

Friedman, I.: Deuterium content of natural waters and other substances, Geochim. Cosmochim. Acta, 4, 89–103, https://doi.org/10.1016/0016-7037(53)90066-0, 1953.

Froehlich, K., Gibson, J. J., and Aggarwal, P.: DEUTERIUM EXCESS IN

https://doi.org/10.5194/egusphere-2023-2058
Preprint. Discussion started: 12 October 2023

PRECIPITATION AND ITS CLIMATOLOGICAL SIGNIFICANCE, 2002.

Gat, J. R.: OXYGEN AND HYDROGEN ISOTOPES IN THE HYDROLOGIC CYCLE, Annu. Rev. Earth Planet. Sci., 1, 225–262, 1996.

Gat, J. R.: Atmospheric water balance?the isotopic perspective, Hydrol. Process., 14, 1357–1369, https://doi.org/10.1002/1099-1085(20000615)14:8<1357::AID-HYP986>3.0.CO;2-7, 2000.

Gat, J. R. and Carmi, I.: Environmental isotopes in the hydrological cycle, J. Geophys. Res., 75, 3039–3048, https://doi.org/10.1029/JC075i015p03039, 2001.

Gat, J. R. and Dansgaard, W.: Stable isotope survey of the fresh water occurrences in Israel and the Northern Jordan Rift Valley, J. Hydrol., 16, 177–211, https://doi.org/10.1016/0022-1694(72)90052-2, 1972.

Gat, J. R., Klein, B., Kushnir, Y., Roether, W., Wernli, H., Yam, R., and Shemesh, A.: Isotope composition of air moisture over the Mediterranean Sea: an index of the air-sea interaction pattern, Tellus B, 55, 953–965, https://doi.org/10.1034/j.1600-0889.2003.00081.x, 2003.

Gimeno, L., Stohl, A., Trigo, R. M., Dominguez, F., Yoshimura, K., Yu, L., Drumond, A., Durán-Quesada, A. M., and Nieto, R.: Oceanic and terrestrial sources of continental precipitation, Rev. Geophys., 50, RG4003, https://doi.org/10.1029/2012RG000389, 2012.

Hoerling, M., Kumar, A., Dole, R., Nielsen-Gammon, J. W., Eischeid, J., Perlwitz, J., Quan, X.-W., Zhang, T., Pegion, P., and Chen, M.: Anatomy of an Extreme Event, J. Clim., 26, 2811–2832, https://doi.org/10.1175/JCLI-D-12-00270.1, 2013.

Hu, L., Luo, J.-J., Huang, G., and Wheeler, M. C.: Synoptic Features Responsible for Heat Waves in Central Africa, a Region with Strong Multidecadal Trends, J. Clim., 32,

https://doi.org/10.5194/egusphere-2023-2058
Preprint. Discussion started: 12 October 2023

7951–7970, https://doi.org/10.1175/JCLI-D-18-0807.1, 2019.

Ingraham, N. L.: Isotopic Variations in Precipitation, in: Isotope Tracers in Catchment Hydrology, Elsevier, 87–118, https://doi.org/10.1016/B978-0-444-81546-0.50010-0, 1998.

Johnson, K. R. and Ingram, B. L.: Spatial and temporal variability in the stable isotope systematics of modern precipitation in China: implications for paleoclimate reconstructions, Earth Planet. Sci. Lett., 220, 365–377, https://doi.org/10.1016/S0012-821X(04)00036-6, 2004.

Jouzel, J., Delaygue, G., Landais, A., Masson-Delmotte, V., Risi, C., and Vimeux, F.: Water isotopes as tools to document oceanic sources of precipitation: Water Isotopes and Precipitation Origin, Water Resour. Res., 49, 7469–7486, https://doi.org/10.1002/2013WR013508, 2013.

Kaakinen, A., Sonninen, E., and Lunkka, J. P.: Stable isotope record in paleosol carbonates from the Chinese Loess Plateau: Implications for late Neogene paleoclimate and paleovegetation, Palaeogeogr. Palaeoclimatol. Palaeoecol., 237, 359–369, https://doi.org/10.1016/j.palaeo.2005.12.011, 2006.

Kathayat, G., Sinha, A., Tanoue, M., Yoshimura, K., Li, H., Zhang, H., and Cheng, H.: Interannual oxygen isotope variability in Indian summer monsoon precipitation reflects changes in moisture sources, Commun. Earth Environ., 2, 96, https://doi.org/10.1038/s43247-021-00165-z, 2021.

Kino, K., Okazaki, A., Cauquoin, A., and Yoshimura, K.: Contribution of the Southern Annular Mode to Variations in Water Isotopes of Daily Precipitation at Dome Fuji, East Antarctica, J. Geophys. Res. Atmospheres, 126, https://doi.org/10.1029/2021JD035397, 2021.

Lau, N.-C. and Nath, M. J.: A Model Study of Heat Waves over North America: Meteorological Aspects and Projections for the Twenty-First Century, J. Clim., 25, 4761–4784, https://doi.org/10.1175/JCLI-D-11-00575.1, 2012.

Leng, M. J. and Marshall, J. D.: Palaeoclimate interpretation of stable isotope data from lake sediment archives, Quat. Sci. Rev., 23, 811–831, https://doi.org/10.1016/j.quascirev.2003.06.012, 2004.

Li, Z.-J., Li, Z.-X., Yu, H.-C., Song, L.-L., and Ma, J.-Z.: Environmental significance and zonal characteristics of stable isotope of atmospheric precipitation in arid Central Asia, Atmospheric Res., 227, 24–40, https://doi.org/10.1016/j.atmosres.2019.04.022, 2019.

McCarroll, D. and Loader, N. J.: Stable isotopes in tree rings, Quat. Sci. Rev., 23, 771–801, https://doi.org/10.1016/j.quascirev.2003.06.017, 2004.

Meehl, G. A. and Tebaldi, C.: More Intense, More Frequent, and Longer Lasting Heat Waves in the 21st Century, Science, 305, 994–997, https://doi.org/10.1126/science.1098704, 2004.

Merlivat, L. and Jouzel, J.: Global climatic interpretation of the deuterium-oxygen 18 relationship for precipitation, J. Geophys. Res., 84, 5029, https://doi.org/10.1029/JC084iC08p05029, 1979.

Miralles, D. G., Teuling, A. J., Van Heerwaarden, C. C., and Vilà-Guerau De Arellano, J.: Mega-heatwave temperatures due to combined soil desiccation and atmospheric heat accumulation, Nat. Geosci., 7, 345–349, https://doi.org/10.1038/ngeo2141, 2014.

Monteiro, J. M. and Caballero, R.: Characterization of Extreme Wet-Bulb Temperature Events in Southern Pakistan, Geophys. Res. Lett., 46, 10659–10668, https://doi.org/10.1029/2019GL084711, 2019.

Patz, J. A., Campbell-Lendrum, D., Holloway, T., and Foley, J. A.: Impact of regional climate change on human health, Nature, 438, 310–317, https://doi.org/10.1038/nature04188, 2005.

https://doi.org/10.5194/egusphere-2023-2058
Preprint. Discussion started: 12 October 2023

Perkins, S. E., Alexander, L. V., and Nairn, J. R.: Increasing frequency, intensity and duration of observed global heatwaves and warm spells, Geophys. Res. Lett., 39, 2012GL053361, https://doi.org/10.1029/2012GL053361, 2012.

Sánchez-Murillo, R., Durán-Quesada, A. M., Esquivel-Hernández, G., Rojas-Cantillano, D., Birkel, C., Welsh, K., Sánchez-Llull, M., Alonso-Hernández, C. M., Tetzlaff, D., Soulsby, C., Boll, J., Kurita, N., and Cobb, K. M.: Deciphering key processes controlling rainfall isotopic variability during extreme tropical cyclones, Nat. Commun., 10, 4321, https://doi.org/10.1038/s41467-019-12062-3, 2019.

Schubert, S. D., Wang, H., Koster, R. D., Suarez, M. J., and Groisman, P. Ya.: Northern Eurasian Heat Waves and Droughts, J. Clim., 27, 3169–3207, https://doi.org/10.1175/JCLI-D-13-00360.1, 2014.

Seneviratne, S. I., Lüthi, D., Litschi, M., and Schär, C.: Land–atmosphere coupling and climate change in Europe, Nature, 443, 205–209, https://doi.org/10.1038/nature05095, 2006.

Sprenger, M., Leistert, H., Gimbel, K., and Weiler, M.: Illuminating hydrological processes at the soil-vegetation-atmosphere interface with water stable isotopes: REVIEW OF WATER STABLE ISOTOPES, Rev. Geophys., 54, 674–704, https://doi.org/10.1002/2015RG000515, 2016.

Thompson, L. G., Yao, T., Mosley-Thompson, E., Davis, M. E., Henderson, K. A., and Lin, P.-N.: A High-Resolution Millennial Record of the South Asian Monsoon from Himalayan Ice Cores, Science, 289, 1916–1919, https://doi.org/10.1126/science.289.5486.1916, 2000.

Turner, J., Lu, H., King, J. C., Carpentier, S., Lazzara, M., Phillips, T., and Wille, J.: An Extreme High Temperature Event in Coastal East Antarctica Associated With an Atmospheric River and Record Summer Downslope Winds, Geophys. Res. Lett., 49, https://doi.org/10.1029/2021GL097108, 2022.

https://doi.org/10.5194/egusphere-2023-2058
Preprint. Discussion started: 12 October 2023

Wang, G., Lan, H., and Liu, Z.: Stable isotope record of super typhoon Lekima (2019), Atmospheric Res., 264, 105822, https://doi.org/10.1016/j.atmosres.2021.105822, 2021.

Wang, S., Zhang, M., Crawford, J., Hughes, C. E., Du, M., and Liu, X.: The effect of moisture source and synoptic conditions on precipitation isotopes in arid central Asia: PRECIPITATION ISOTOPES IN CENTRAL ASIA, J. Geophys. Res. Atmospheres, 122, 2667–2682, https://doi.org/10.1002/2015JD024626, 2017.

Wehrli, K., Guillod, B. P., Hauser, M., Leclair, M., and Seneviratne, S. I.: Identifying Key Driving Processes of Major Recent Heat Waves, J. Geophys. Res. Atmospheres, 124, 11746–11765, https://doi.org/10.1029/2019JD030635, 2019.

Wei, Z., Lee, X., Liu, Z., Seeboonruang, U., Koike, M., and Yoshimura, K.: Influences of large-scale convection and moisture source on monthly precipitation isotope ratios observed in Thailand, Southeast Asia, Earth Planet. Sci. Lett., 488, 181–192, https://doi.org/10.1016/j.epsl.2018.02.015, 2018.

Zhu, G., Sang, L., Zhang, Z., Sun, Z., Ma, H., Liu, Y., Zhao, K., Wang, L., and Guo, H.: Impact of landscape dams on river water cycle in urban and peri-urban areas in the Shiyang River Basin: Evidence obtained from hydrogen and oxygen isotopes, J. Hydrol., 602, 126779, https://doi.org/10.1016/j.jhydrol.2021.126779, 2021.

Zhu, G., Yong, L., Zhao, X., Liu, Y., Zhang, Z., Xu, Y., Sun, Z., Sang, L., and Wang, L.: Evaporation, infiltration and storage of soil water in different vegetation zones in the Qilian Mountains: a stable isotope perspective, Hydrol. Earth Syst. Sci., 26, 3771–3784, https://doi.org/10.5194/hess-26-3771-2022, 2022a.

Zhu, G., Liu, Y., Shi, P., Jia, W., Zhou, J., Liu, Y., Ma, X., Pan, H., Zhang, Y., Zhang, Z., Sun, Z., Yong, L., and Zhao, K.: Stable water isotope monitoring network of different water bodies in Shiyang River basin, a typical arid river in China, Earth Syst. Sci. Data, 14, 3773–3789, https://doi.org/10.5194/essd-14-3773-2022, 2022b.

https://doi.org/10.5194/egusphere-2023-2058
Preprint. Discussion started: 12 October 2023

Zhu, G., Liu, Y., Wang, L., Sang, L., Zhao, K., Zhang, Z., Lin, X., and Qiu, D.: The isotopes of precipitation have climate change signal in arid Central Asia, Glob. Planet. Change, 225, 104103, https://doi.org/10.1016/j.gloplacha.2023.104103, 2023.